Model for the Transition to the Radiatively Improved Mode in a Tokamak

M. Z. Tokar,[1] J. Ongena,[2] B. Unterberg,[1] and R. R. Weynants[2]

[1]*Institut für Plasmaphysik, Forschungszentrum Jülich GmbH, EURATOM Association, D-52425 Jülich, Germany*

[2]*Laboratoire de Physique des Plasmas–Laboratorium voor Plasmafysica, "Association EURATOM–Belgian State," Ecole Royale Militaire–Koninklijke Militaire School, B-1000, Brussels, Belgium*

(Partners in the Trilateral Euregio Cluster)

(Received 20 May 1999)

A model for the transition to the radiatively improved (RI) mode triggered in tokamaks by seeding of impurities is proposed. This model takes into account that with increasing plasma effective charge the growth rate of the toroidal ion temperature gradient (ITG) instability, considered nowadays as the dominant source of anomalous energy losses in low-confinement (L) mode, decreases. As a result the plasma density profile peaks due to an inward convection generated by trapped electron turbulence. This completely quenches ITG induced transport and a bifurcation to the RI mode occurs. Conditions necessary for the L-RI transition are investigated.

PACS numbers: 52.35.Py, 52.55.Fa

The regimes of tokamak operation with transport of energy and particles reduced by seeding of impurities have been obtained in different devices, e.g., in ISX-B [1], ASDEX [2], TEXTOR [3], ASDEX-U [4], TFTR [5], and DIII-D [6]. In these experiments a deliberate pollution of the plasma by impurities, e.g., by neon, argon, krypton, xenon, led to an improvement in the energy confinement in spite of increased radiation losses. Understanding of physical processes responsible for such a surprising effect of impurities can bring a new insight into the nature of anomalous transport and mechanisms responsible for the turbulence suppression.

An analysis of data from TEXTOR-94 [7] allowed one to unify the scalings established for the energy confinement time in radiatively improved (RI) and linear Ohmic confinement (LOC) modes through a suitable normalization of the discharge parameters. This substantiated the idea that in both regimes the transport is of the same nature and originates from the dissipative trapped electron (DTE) instability [8]. This instability was identified before as the most important one under LOC conditions [9,10]. The more dangerous toroidal ion temperature gradient (ITG) instability, which causes deterioration of confinement in saturated Ohmic (SOC) and low (L) confinement modes, is quenched in the LOC case due to a rather peaked density profile [10]. Recent investigations have shown that also in the RI mode in TEXTOR-94 ITG turbulence is suppressed in a noticeable plasma region owing to the density peaking [11,12], and a weaker DTE transport determines the energy losses.

In spite of this improved understanding, the transport mechanism responsible for the density peaking, which is the key process for the L-RI transition, remained unclear. In this Letter a possible scenario is presented which can be briefly described as follows. Seeding of impurities leads to an increase in the plasma effective charge Z_{eff}. As a result the velocity of the ion diamagnetic drift decreases and the growth rate of ITG instability reduces [12]. Therefore DTE modes become more important and force the plasma to a state where in the absence of a sizable particle source the product of the electron density n and the safety factor q is constant over the plasma [13,14]. For q profiles with a positive shear typical for the RI mode this leads to a density peaking. The growth rate of the ITG instability decreases further and a bifurcation to a new state with a reduced transport governed by DTE turbulence takes place. To find the conditions necessary for such a bifurcation a simple transport model will be elaborated here which takes into account diffusive and convective (pinch) contributions to the electron flux from both ITG and DTE unstable modes.

In comparing our results with experimental observations we shall refer to a discharge in TEXTOR-94 where the L-RI transition was caused by seeding of neon. Figure 1 shows the measured profiles of the main plasma parameters in this discharge and the q profile calculated by the code RITM [3].

For plasmas of not very low collisionality, typical for L and RI regimes, ITG and DTE modes can be characterized by individual linear growth rates γ [15]. In the present Letter we confine ourselves to a qualitative analysis and use approximate analytical expressions for γ-s. Applying the model from Ref. [12] we obtain in the ITG case

$$\gamma_{\text{ITG}} \approx \frac{2cT_e k_\theta}{eBR}\sqrt{\frac{\varepsilon_i}{Z_{\text{eff}}}(1 - 0.67p) - \frac{\varepsilon_i^2}{4}p^2}. \quad (1)$$

Here $T_{e,i}$ are the electron and ion temperatures whose gradients are characterized by $\varepsilon_{e,i} = -(R/2)(d\ln T_{e,i}/dr)$, where R and r are the major and minor radii, respectively; for the poloidal component of the wave vector we assume the value $k_\theta \approx 1/2\rho_s$, where ρ_s is the Larmor radius of deuterons, at which γ_{ITG} approaches its maximum when polarization drift and gyroviscosity are taken into account [12].

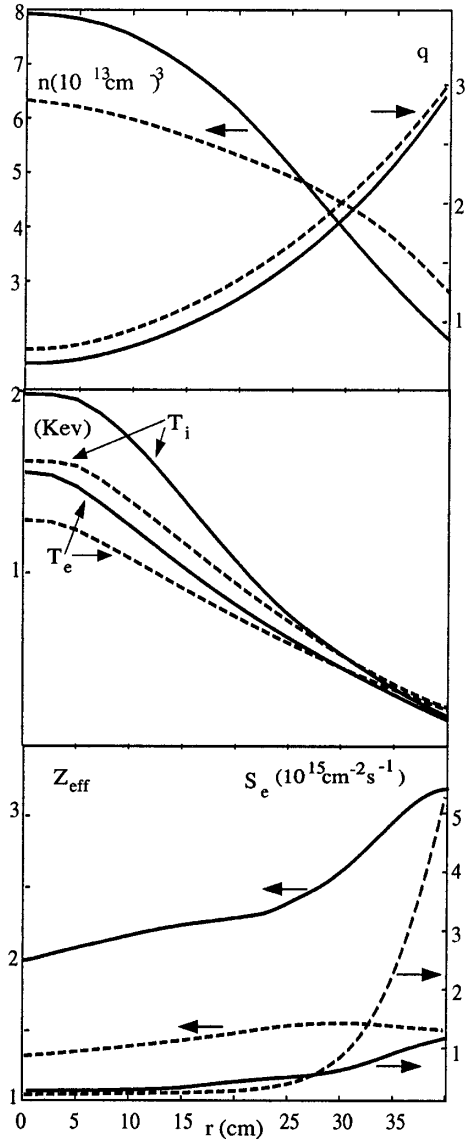

FIG. 1. Plasma parameters in the L mode (time $t = 1.5$ s, broken lines) and RI mode ($t = 2$ s, solid lines) stages of shot 68 803 in TEXTOR-94: electron density n, safety factor q, electron and ion temperatures $T_{e,i}$, effective ion charge Z_{eff}, and electron source density S_e.

Instead of the parameter $\eta_i = d\ln T_i/d\ln n$, normally used to analyze the ITG modes, the *peaking factor* $p \equiv 1/\eta_i$ is introduced in Eq. (1). One can see that γ_{ITG} decreases with increasing p and reduces to zero when p approaches $p_* = (2/\varepsilon_i)[\sqrt{(0.67^2/Z_{\text{eff}}^2) + (\varepsilon_i/Z_{\text{eff}})} - (0.67/Z_{\text{eff}})]$. This critical level becomes lower when Z_{eff} is growing by impurity seeding.

Conversely to the ITG instability, the growth rate of the DTE modes increases with the density peaking [8,16],

$$\gamma_{\text{DTE}} \approx 8\left(\frac{cT_e k_\theta}{eBR}\right)^2 \frac{r}{R} f_{\text{tr}} \frac{\varepsilon_i \epsilon_e}{\nu_e} p\,, \tag{2}$$

where ν_e and f_{tr} are the frequency of electron collisions and fraction of trapped particles, respectively.

To describe the behavior of the peaking factor p we proceed from the continuity equation for electrons:

$$\frac{\partial n}{\partial t} + \frac{1}{r}\frac{\partial}{\partial r}(r\Gamma) = S_e\,. \tag{3}$$

Here the electron flux density includes contributions from ITG and DTE types of turbulence, $\Gamma = \Gamma_{\text{ITG}} + \Gamma_{\text{DTE}}$, and S_e is the electron source due to (i) ionization of deuterium atoms from neutral beams and recycling at the plasma edge and (ii) ionization of impurities (see Fig. 1).

Both Γ_{ITG} and Γ_{DTE} have diffusive and convective (pinch) components proportional to the gradients of the density and other parameters, respectively. In the case of an ion driven turbulence, e.g., due to ITG instability, the pinch component is relatively weak [14,17,18] and will be neglected henceforth:

$$\Gamma_{\text{ITG}} \approx -D_\perp^{\text{ITG}} \times \frac{\partial n}{\partial r}\,. \tag{4}$$

For the electron flux generated by DTE turbulence we assume according to Ref. [14]

$$\Gamma_{\text{DTE}} \approx -D_\perp^{\text{DTE}} \times \left(\frac{\partial n}{\partial r} + \frac{\partial \ln q}{\partial r} n\right). \tag{5}$$

The pinch component here is due to the energy transfer from unstable waves to trapped electrons. Because of conservation of the second invariant this causes a motion of trapped particles to low q and the DTE turbulence involves transit particles into this motion too. The physics of this phenomenon is explained in [13,14]. In the absence of an electron flux, Eq. (5) results in $nq \approx$ const.

The particle transport due to the instabilities under consideration is automatically ambipolar since it results from drifts due to fluctuating electric fields. This implies that the diffusivities of electrons, the main ions, and the impurities are close to each other. To estimate those a "mixing length" limit [15] will be applied:

$$D_\perp \sim \frac{\gamma}{k_\theta^2} q^2. \tag{6}$$

The factor q^2 allows one to match $D_\perp$ to the experimentally observed increase in transport coefficients toward the plasma edge [19]. There are also theoretical reasons in favor of introduction of such a factor [20].

According to Eq. (4), the particle transport caused by the ITG turbulence results in a flat density profile in the plasma core where the particle source and Γ are small. This agrees with observations in the L mode. When the ITG instability is quenched, DTE turbulence produces a relatively strong inward convection for a conventional q profile with a positive shear. That can explain the density peaking during the L-RI transition.

Under stationary conditions the integral of Eq. (3) results in an equation for the peaking factor p,

$$G(p) \equiv \Gamma - \frac{1}{r}\int_0^r S_e r\, dr = 0\,. \tag{7}$$

With the help of Eqs. (1)–(6) one gets

$$G(p) = \Gamma_0 p\left[\sqrt{\frac{1 - 0.67p}{\varepsilon_i Z_{\text{eff}}} - \frac{p^2}{4}} + \left(\frac{r}{R}\right)^{3/2}\frac{\varepsilon_e c_s}{\nu_e R}\left(p - \frac{d\ln q}{d\ln T_i}\right)\right] - \frac{1}{r}\int_0^r S_e r\, dr\,, \tag{8}$$

where $\Gamma_0 = 8nc_s(\varepsilon_i\rho_s/R)^2$ and $c_s = \sqrt{T_e/m_i}$.

The function $G(p)$ is shown in Fig. 2 for typical values of parameters in the L- and RI-mode discharges at $r = 30$ cm, where the difference in the density gradients is the most pronounced. External parameters such as Z_{eff} were evaluated from the profiles in Fig. 1, e.g., the temperature profiles were used to quantify $\varepsilon_{e,i}$.

The form of $G(p)$ can be explained as follows. For $p < p_*$ ITG-induced diffusion makes the main contribution to Γ. This contribution is proportional both to the density gradient, i.e., p, and to $D_\perp^{\text{ITG}}$. The latter decreases with the peaking factor and this provides a maximum in $G(p)$. For $p > p_*$ only DTE transport contributes to Γ and the latter increases monotonically with the peaking factor.

Because of Z_{eff} dependence in γ_{ITG} the maximum value of G, $G_{\max}$, decreases with increasing Z_{eff}. For L-mode conditions with a low Z_{eff}, $G_{\max} > 0$ and there are two stable stationary states. The one with the smallest p has a high level of ITG turbulence so that the diffusive flux dominates the convective one and provides the necessary stationary flow at a low density gradient. The time evolution of the entire density profile determines that namely this state, and not that with the highest p, is realized in the experiment. This was confirmed by a numerical integration of Eq. (3) for realistic boundary and initial conditions (see below). In the RI-mode case $G_{\max} < 0$ and only the state where ITG instability is quenched survives. The stationary values of p which follow from Fig. 2 are close to the experimental ones (0.37 and 0.76 for L- and RI-mode conditions, respectively).

When Z_{eff} increases during the seeding of impurity, there is a critical situation for which $G_{\max} = 0$. After this a spontaneous density peaking sets in and a bifurcation into the state with completely suppressed ITG transport takes place. To find the critical conditions we have assumed that all parameters in the function G, excluding p, vary with Z_{eff} as Z_{eff}^{β}. The exponents β were chosen to reproduce the magnitudes which correspond to profiles in Fig. 1. Then Eq. (8) has been solved for different values of Z_{eff} and the found dependence of the transport coefficients $D_\perp^{\text{ITG}}$, $D_\perp^{\text{DTE}}$, and $D_\perp^{\text{an}} = D_\perp^{\text{ITG}} + D_\perp^{\text{DTE}}$ is shown in Fig. 3. The sharp transition at $Z_{\text{eff}} \approx 2$ leads to a drop in the effective transport coefficients in agreement with TRANSP modeling [7].

The shape of the density profile before and after the L-RI transition has been simulated by a numerical integration of the continuity equation (3). The integration domain was restricted to $0 < r < 40$ cm, because at the plasma edge, i.e., for $r > 40$ cm, ITG and DTE instabilities are supposed not to be the main causes of anomalous transport [21]. The density measured at $r = 40$ cm has been taken as a boundary condition. As a preliminary step, a steady state solution has been found with the radial profiles of the ion effective charge, ion and electron temperatures, safety factor, and electron source measured in the L mode (broken curves in Fig. 1). Then these parameters were changed instantaneously to their level in the RI mode (solid curves in Fig. 1) and the evolution of n caused by this change has been simulated. In Fig. 4 the density profiles measured in shot 68 803 in the L-mode state at $t = 1.5$ s, i.e., immediately before neon puffing, and at $t = 2$ s after the L-RI transition are compared with the asymptotically ($t \to \infty$) calculated profiles. The agreement between the measured and simulated profiles shows that the proposed

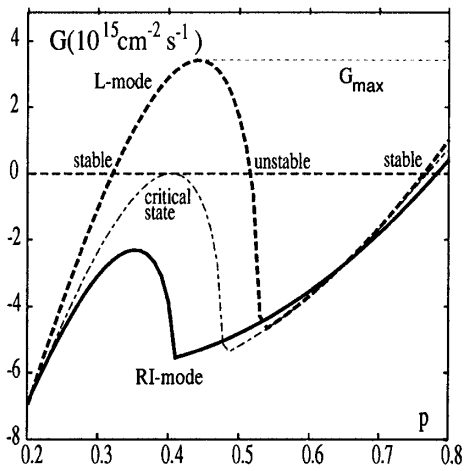

FIG. 2. The value G versus the peaking factor p.

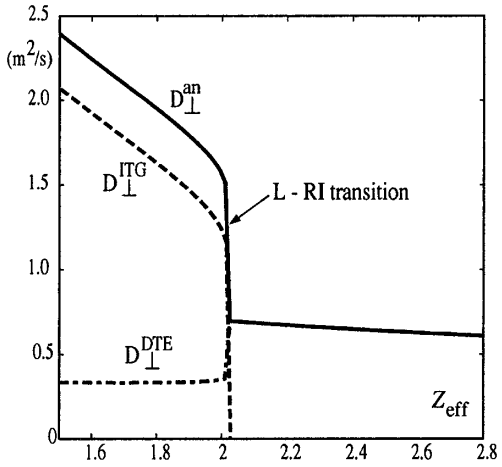

FIG. 3. The dependence of transport coefficients on the plasma effective charge.

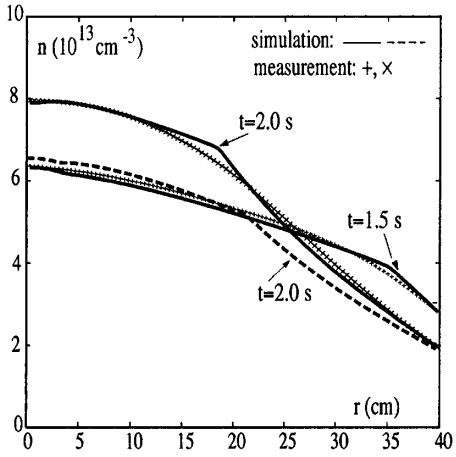

FIG. 4. Computed and experimental profiles of the electron density; the broken curve is obtained with Z_{eff} kept at the L-mode level.

model gives a good description of the particle transport in both operational regimes.

To prove that the increase in the ion effective charge is probably the most important factor leading to the L-RI transition, Eq. (3) has been integrated with Z_{eff} kept at the L-mode level while other parameters were changed to their magnitudes in the RI mode. The result demonstrated in Fig. 4 by the broken curve confirms that no density peaking occurs in this case. This can explain why other methods used for cooling of the plasma edge, e.g., an intensive puffing of the main gas, does not lead to an improvement of confinement. The importance of the ion effective charge is also confirmed by results from TFTR [5], where a significant reduction of the ion energy transport was achieved by the seeding of xenon and krypton which radiate at all plasma radii.

The present model for the suppression of the ITG turbulence during the L-RI transition is based on the interplay between diffusive and convective components of the particle flows. For the edge and internal barriers where reduction in the transport is attributed to sheared $\mathbf{E} \times \mathbf{B}$ rotation [22] only particle diffusion is taken normally into account. Our calculations show that this mechanism cannot trigger a transition to the RI mode, where transport is improved in a significant part of the plasma volume and profiles are not extremely steep anywhere. After the L-RI transition the radial electric field contributes noticeably to the reduction of transport in discharges with a fast toroidal rotation induced by unbalanced neutral injection [12,23,24].

In concluding, we note that the present approach provides also an explanation for the transition between LOC and SOC confinement modes caused by increase in the plasma density. Indeed, the DTE contribution to the electron flux is inversely proportional to ν_e and, thus, to n. If the latter exceeds a critical level the convective flux becomes too small, the density profile flattens, and the ITG transport drastically increases.

The authors thank R. Sydora for fruitful discussions and R. Jaspers, H. R. Koslowski, A. Krämer-Flecken, A. M. Messiaen, and the TEXTOR-94 team for valuable experimental data.

[1] E. A. Lazarus *et al.*, J. Nucl. Mater. **121**, 61 (1984).
[2] M. Bessenroth-Weberpals *et al.*, Nucl. Fusion **31**, 155 (1991).
[3] J. Ongena *et al.*, Phys. Scr. **52**, 449 (1995).
[4] J. Neuhauser *et al.*, Plasma Phys. Controlled Fusion **37**, A37 (1995).
[5] K. W. Hill *et al.*, Phys. Plasmas **6**, 877 (1999).
[6] G. L. Jackson *et al.*, J. Nucl. Mater. **266–269**, 380 (1999).
[7] R. R. Weynants *et al.*, Nucl. Fusion **39**, 1637 (1999).
[8] B. B. Kadomtsev and O. P. Pogutse, Nucl. Fusion **11**, 67 (1971).
[9] F. Romanelli *et al.*, Nucl. Fusion **26**, 1515 (1986).
[10] R. R. Dominguez and R. E. Waltz, Nucl. Fusion **27**, 65 (1987).
[11] R. Sydora (private communication).
[12] M. Z. Tokar *et al.*, Plasma Phys. Controlled Fusion **41**, L9 (1999).
[13] V. V. Yankov and J. Nycander, Phys. Plasmas **4**, 2907 (1997).
[14] D. R. Baker and M. N. Rosenbluth, Phys. Plasmas **5**, 2936 (1998).
[15] W. Horton, Rev. Mod. Phys. **71**, 735 (1999).
[16] J. Nilsson and J. Weiland, Nucl. Fusion **34**, 803 (1994).
[17] R. R. Dominguez, Phys. Fluids B **5**, 1782 (1993).
[18] M. B. Isichenko, A. V. Grusinov, and P. H. Diamond, Phys. Rev. Lett. **74**, 4436 (1995).
[19] A. Taroni, M. Erba, E. Springmann, and F. Tibone, Plasma Phys. Controlled Fusion **36**, 1629 (1994).
[20] A. Rogister, Phys. Plasmas **2**, 2729 (1995).
[21] A. Zeiler, D. Biskamp, J. F. Drake, and B. N. Rogers, Phys. Plasmas **5**, 2654 (1998).
[22] G. M. Staebler, Plasma Phys. Controlled Fusion **40**, 569 (1998).
[23] M. Z. Tokar *et al.*, Nucl. Fusion **38**, 961 (1998).
[24] G. M. Staebler *et al.*, Phys. Rev. Lett. **82**, 1692 (1999).